CRCLEME
Cooperative Research Centre for Landscape Environments and Mineral Exploration

action Salinity & Water AUSTRALIA

Government of South Australia

OPEN FILE REPORT SERIES

CSIRO

Australian Government Geoscience Australia

OTBC

CALIBRATION OF RESOLVE AIRBORNE ELECTROMAGNETIC DATA - RIVERLAND AND EAST TINTINARA, SOUTH AUSTRALIA

R. Brodie, A. Green and T. Munday

CRC LEME OPEN FILE REPORT 173

September 2004

CRCLEME

CALIBRATION OF RESOLVE AIRBORNE ELECTROMAGNETIC DATA - RIVERLAND AND EAST TINTINARA, SOUTH AUSTRALIA

R. Brodie, A. Green and T. Munday

CRC LEME OPEN FILE REPORT 173

September 2004

Report prepared for the South Australia Salinity Mapping and Management Support Project.
This project is jointly funded by the South Australian and Commonwealth Governments under the National Action Plan for Salinity and Water Quality.

CRC LEME is an unincorporated joint venture between CSIRO-Exploration & Mining, and Land and Water, The Australian National University, Curtin University of Technology, University of Adelaide, Geoscience Australia, Primary Industries and Resources SA, NSW Department of Mineral Resources and Minerals Council of Australia.

Headquarters: CRC LEME c/o CSIRO Exploration and Mining, PO Box 1130, Bentley WA 6102, Australia

Copies of this Publication can be obtained from :
The publications Officer, CRCLEME, c/- CSIRO Exploration and Mining, PO Box 1130, Bentley WA 6120, Australia. Information on other publications in this series may be obtained from the above, or from http://crcleme.org.au
Cataloguing-in-Publication:
Name: Brodie, R., Green, A. and Munday, T. Title: Calibration of RESOLVE airborne electromagnetic data – Riverland and East Tintinara, South Australia
ISBN 1 921039 11 6
1. Riverland and East Tintinara, South Australia 2. AEM 3. Calibration I. Name II. Title
CRCLEME Open File Report 173
ISSN 1329-4768

Address and Affiliation of Authors

Ross Brodie
Geoscience Australia
GPO Box 378,
Canberra, ACT 2601
Australia

Andy Green
OTBC Pty. Ltd
8 Lawley Cres.
Pymble NSW 2073
Australia

Tim Munday
Cooperative Research Centre for Landscape Environments and Mineral Exploration
c/- CSIRO Exploration and Mining
26 Dick Perry Avenue,
Technology Park,
Kensington, Western Australia 6151
Australia.

PREFACE AND EXECUTIVE SUMMARY

This project is a subset of the Riverland and Tintinara projects in South Australia conducted under the auspices of the South Australian Salinity Mapping and Monitoring Project. The decision of the SA-Salinity Mapping and Monitoring Support Project to employ a frequency domain helicopter EM system for mapping near surface conductivity related to the presence of clay-rich materials came with an expectation that the careful monitoring of system performance would be an essential prerequisite to ensuring data of a consistent quality appropriate for inversion.

The activity reported here was conducted to assist the application of a constrained inversion technique with RESOLVE helicopter EM data in order to map the location and thickness of the near-surface clay-rich units in the Riverland and Tintinara East areas in South Australia. It is believed that this clay acts to delay groundwater recharge where present. The RESOLVE system has very wide bandwidth (100 KHz to 400Hz) although it does not sample this frequency range in great detail. This under-sampling of the full frequency response means that it is more difficult to invert the data to a complete vertical conductivity profile.

Accurate inversion depends on having correctly calibrated data. Correctly calibrated data is most essential for this project because the accurate location of near surface conductive units is dependent on subtle changes in the high-frequency response. This report describes the calibration procedures used to process the data delivered by the contractor, and was always planned as an integral part of the project.

Dr. Tim Munday
Project Leader
December 2003

CONTENTS

FIGURES

TABLES

ABSTRACT

The good calibration of airborne electromagnetic data, using a combination of ground EM and borehole conductivity measurements, is critical to obtaining accurate conductivity-depth models. This is particularly so for helicopter frequency domain EM data where calibration and other errors can have a significant effect on the results of inversion. Minimisation of calibration errors in HEM data has become a more important issue as we have evolved from the use of apparent conductivities (resistivity) to the use of pseudo sections, multi-layer inversions fast approximate imaging methods such as CDI's.

In this study, conducted using RESOLVE HEM data for the Riverland and Tintinara East regions of South Australia, our intent was to better map a near-surface conductor associated with clay-rich sediments. Accurate calibration of the high frequency data was particularly important in this regard. Down-hole induction conductivity log information has been used to calibrate for the Riverland and Tintinara East surveys conducted in South Australia. Numerical forward modelling using the drill hole results and the observed HEM bird altitude has shown that the observed responses at each frequency should be multiplied by the following factors in order to match the expected ground responses.

Frequency (Hz)	385	1518	3323	6135	25380	106140
Calibration Factor	0.96	1.04	1.11	1.15	1.29	1.23

1. INTRODUCTION

1.1 Background

Determining the spatial distribution and variability (including thickness) of near-surface clay-rich sediments formed a critical part of the SA-Salinity Mapping and Monitoring Support Project's activities in Riverland and Tintinara. Previously, our knowledge of these attributes was limited to scattered drillholes and outcrop. More reliable and detailed predictions of the effects of particular management options on recharge require this information at a resolution which was only likely if we were to employ an airborne electromagnetic (AEM) system. Where present, these clays are characterised by elevated conductivities relative to overlying and underlying sedimentary units.

A carefully considered forward modelling strategy was designed to verify whether these materials could be mapped and if so what system, if any, was best for these purposes (Munday *et al.*, 2002). These studies suggested that a frequency domain HEM, namely the RESOLVE system, was the best mapping option for the target concerned. However, at the outset, we recognised that to accurately map near surface conductivity variations associated with the clays required good calibration of the airborne electromagnetic data. This was regarded as vital to obtaining accurate conductivity-depth models, particularly so for helicopter frequency domain EM data. Poor coil-calibration and other errors such as system drift can have a significant effect on the results of inversion, because the inversion of electromagnetic data is essentially a type of differencing process, with small errors in these data magnifying to much larger errors in the values of the parameters that result from the inversion process.

Previous experience with multi-coil frequency domain airborne EM systems has indicated that they often require calibration to produce a consistent data suitable for inversion. Deszcz-Pan *et al*. (1988) discuss the issue, review previous calibration efforts and present a calibration procedure for a DIGHEM (a similar EM system to the RESOLVE) survey conducted on the coast of Florida. There, the ground has a well-stratified conductivity structure, but they found that, in order to obtain satisfactory inversion results, it was necessary to recalibrate the data based on ground geophysical measurements. For these reasons we always planned to incorporate a data checking and calibration phase in the Riverland and Tintinara project, using a limited number of ground TEM soundings and borehole EM induction logs located within the survey areas, following a similar strategy to the one they described. The approach described here also builds on procedures developed for the calibration of AEM data using borehole data as discussed in Lane *et al.*, (2001) and Brodie *et al.*, (2003).

It must be stressed that the calibration procedure discussed here is in addition to that performed before the contractor, Fugro Airborne Surveys, delivered the data. The details of these calibration procedures can be found in Fugro Acquisition and Processing Report for the Riverland and Tintinara Surveys (Cowey *et al.*, 2003).

1.2 Study Areas

The Riverland survey area is located along the southern bank of the River Murray between Renmark, Loxton and Kingston on Murray. The Tintinara study area, located in the south-east of the State near Keith, was divided into two adjacent survey areas; East and West. We have only considered the calibration of data from the Riverland and Tintinara East data sets in this study (Figure 1), particularly as the target is similar in both survey areas. Nonetheless, the results described here are likely to be applicable to the calibration of the Tintinara West data set.

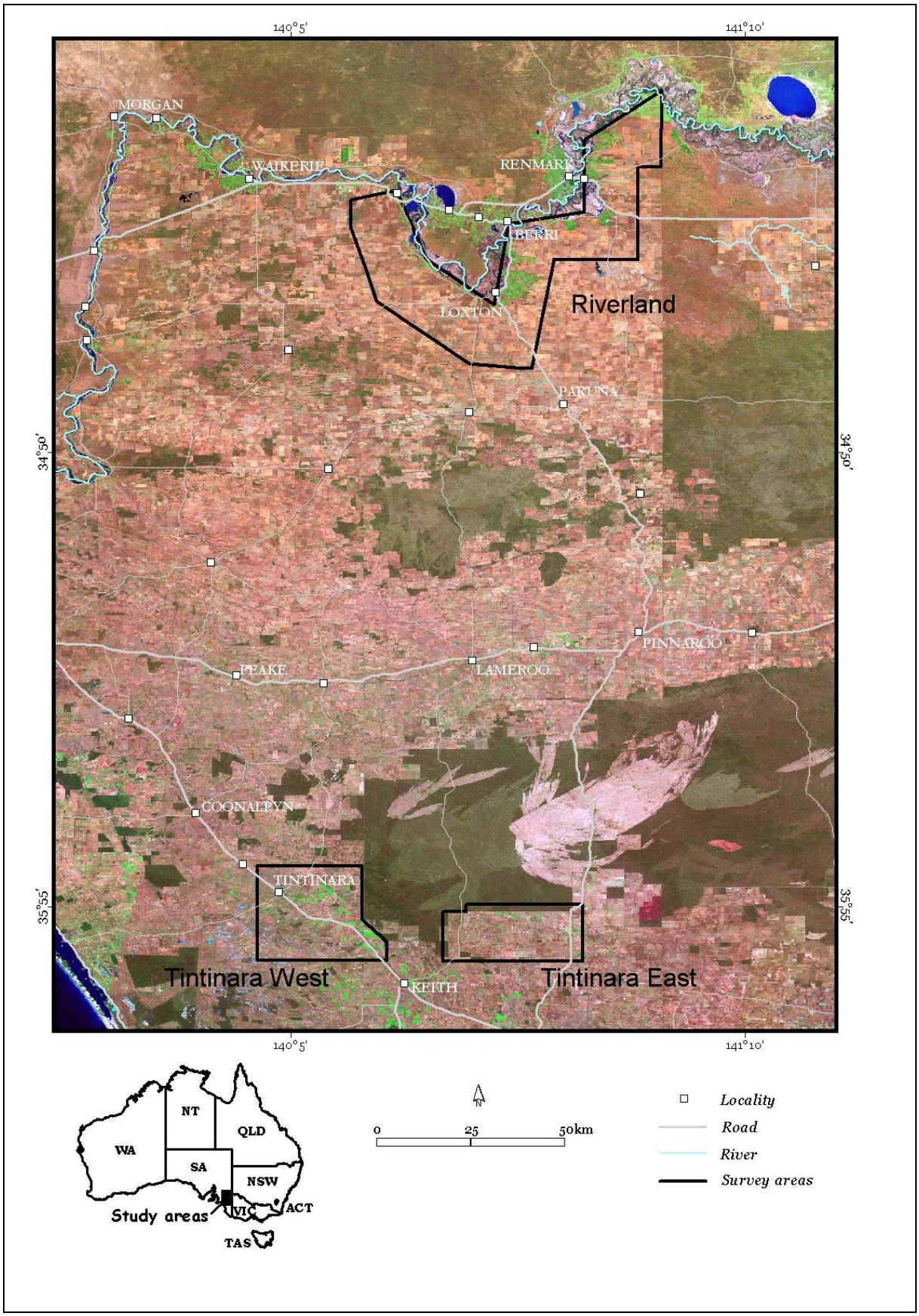

Figure 1.: Location of Riverland and Tintinara RESOLVE survey areas overlain on a Landsat TM colour composite image.

2. RESOLVE HELICOPTER EM SYSTEM

The RESOLVE helicopter electromagnetic (HEM) system is a six frequency EM system that makes use of transmitter and receiver coils housed in a torpedo-shaped tube called a bird that is towed beneath a helicopter. The bird is approximately 9 m long and is slung 30 m below the helicopter (see Figure 2). During surveying the bird is flown 30 m above the land surface. Using six different frequency-coil-pair combinations, the electromagnetic response is measured as a function of frequency. Data are acquired about every 3 m along flight lines.

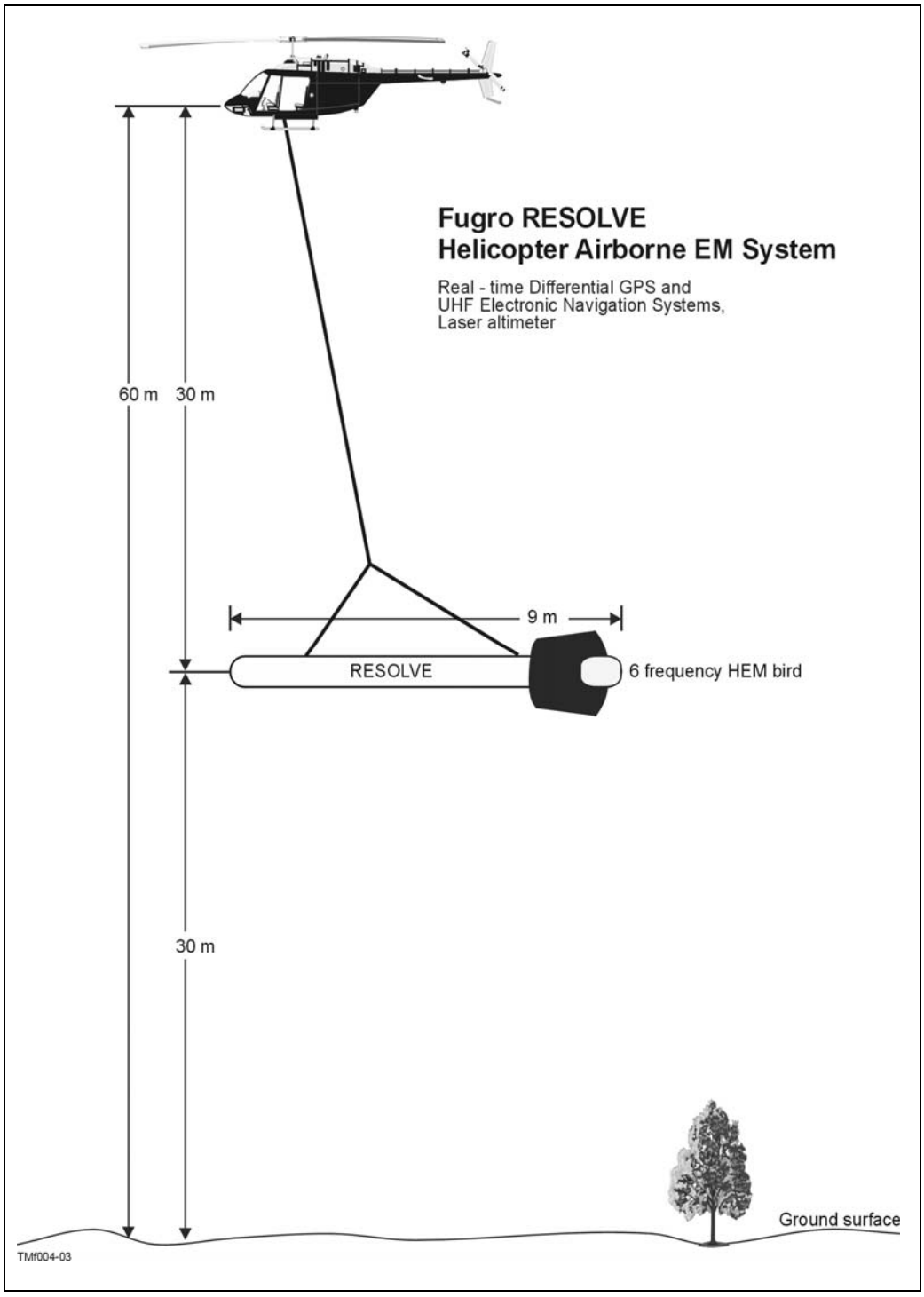

Figure 2.: RESOLVE HEM survey configuration

Details of the RESOLVE HEM system are summarised in Tables 1 and 2. The RESOLVE bird contains five horizontal coplanar coils, and in the South Australian surveys measured an EM response at 385Hz, 1518Hz, 6135Hz, 25380Hz and 106140 Hz (Table 2), configured as shown in Figure 3. It also has one coaxial coil pair which measured a response at 3323Hz.

Table 1. Summary of RESOLVE HEM system characteristics for the Riverland and Tintinara surveys.

Number of coil sets	6
Navigation	Real time differential GPS mounted on helicopter Ashtech Glonass GG24
Positioning	Post processed GPS mounted on bird Dual-frequency Ashtech Z-Surveyor 1.0 second sample rate
Altimeters	Radar altimeters mounted on helicopter, Sperry RT220 Laser altimeter mounted in bird, Optech G150 0.1 second sample rate
Electromagnetic sampling	6 inphase channels at 0.1 second sample rate 6 quadrature channels at 0.1 second sample rate
Monitor Channels	Horizontal coplanar sferics at 0.1 second sample rate Horizontal coplanar powerline at 0.1 second sample rate Vertical coaxial sferics at 0.1 second sample rate Vertical coaxial powerline at 0.1 second sample rate

Table 2. Summary of RESOLVE coil sets.

Frequency (Hz)	Separation (m)	Orientation	Additive Inphase Noise (Std Dev) Estimate (ppm)	Additive Quadrature Noise (Std Dev) Estimate (ppm)	Multiplicative Inphase Noise (Std Dev) Estimate (%ppm)	Multiplicative Quadrature Noise (Std Dev) Estimate (%ppm)
385	7.86	HCP	2.55	1.5	1.2	1.85
1518	7.86	HCP	4.15	1.9	1.6	2.35
3323	8.99	VCX	2.9	1.5	1.9	2.7
6135	7.86	HCP	5.15	3.2	1.85	2.6
25380	7.86	HCP	8.5	6.65	2.1	2.7
106140	7.86	HCP	13.8	10.4	2.15	2.45

Note: HCP = Horizontal coplanar; VCX = Vertical coaxial

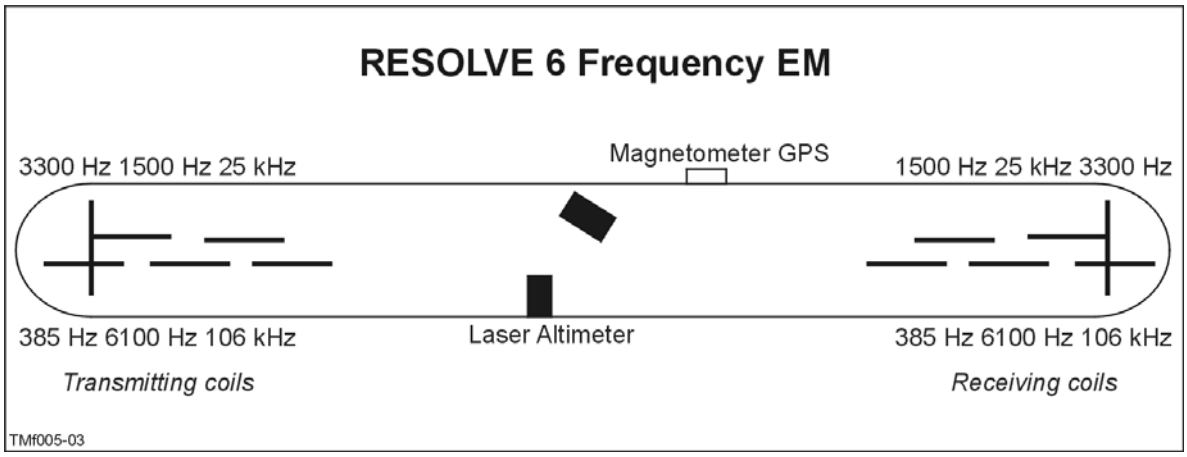

Figure 3.: Coil configuration in the RESOLVE bird

The RESOLVE is a fully digital EM system, offering improved signal:noise characteristics compared with previous HEM systems (e.g. DIGHEM), real-time signal processing as well as internal calibration coils for automatic phase and gain calibration in the air. These characteristics arguably result in higher accuracy and a reduced drift (Cowey *et al.*, 2003). The very high frequencies help resolve very near surface conductors as might be represented by the clay-rich near-surface materials found in Riverland and Tintinara. Decreasing the frequency increases the depth of exploration

3. DATA ACQUISITION AND PROCESSING

3.1 Data acquisition

Survey parameters for the two study areas are described in Table 3. Further details of the data acquisition and processing are provided in the survey Acquisition and Processing Report (Cowey *et al* 2003).

Table 3: Summary of Riverland and Tintinara RESOLVE HEM survey specifications.

Contracting Organisation	Bureau of Rural Sciences
Client	SA-SMMSP
Contract Supervision Organisation	Geoscience Australia
Survey Company	Fugro Airborne Surveys Pty Ltd
Fugro Airborne Surveys Job Number	1543 – Riverland 1543 – Tintinara East and West
Dates Flown	26/06/2002 – 26/06/2002 – Riverland 15/07/2002 – 15/08/2002 -Tintinara
Aircraft	AS-350BA Squirrel, VH-RTV
EM System	RESOLVE
Nominal Terrain Clearance	Helicopter 60 metres Towed bird assembly 30 metres
Total Line Kilometres	11,476 kilometres - Riverland 2,133 kilometres – Tintinara West 1,669 kilometres – Tintinara East
Traverse Line Spacing	150/300 metres – Riverland 300 metres – Tintinara East and West
Traverse Line Direction	0° - 180° – Riverland 90° – 270° – Tintinara East and West
Tie Line Spacing	4 to 6 kilometres (variable)
Tie Line Direction	90° - 270° – Riverland 0° - 180° – Tintinara East and West

3.2 Data processing

The measured electromagnetic response from a frequency domain HEM system consists of two parts, one which is in phase with the transmitted signal and the other which is out of phase (quadrature component) with respect to the transmitted signal. The response is measured in parts per million of the transmitted signal and is commonly converted to an apparent conductivity or resistivity to facilitate comparison of data from different locations (Fitterman and Deszcz-Pan, 2001).

The *Apparent Resistivity, or Apparent Conductivity* is the resistivity/conductivity of a homogeneous half-space required to produce the measured response. Given that in normal situations, the response is measured over a heterogeneous earth rather than a homogeneous one, and we use the term "apparent" to describe the observed electrical property. An apparent resistivity/conductivity is computed for each frequency. An apparent resistivity/conductivity image alone does not provide any depth information; however, by comparison of images made using different transmitter frequencies some idea of how conductivity varies with depth can be formed. To determine true conductivity variation with depth the data must be modeled. This entails taking data from each measurement point or fiducial along a flight line, consisting of the electromagnetic response at several frequencies, and estimating the parameters of a layered-earth, conductivity- depth model, that would produce the observed response (Figure 4).

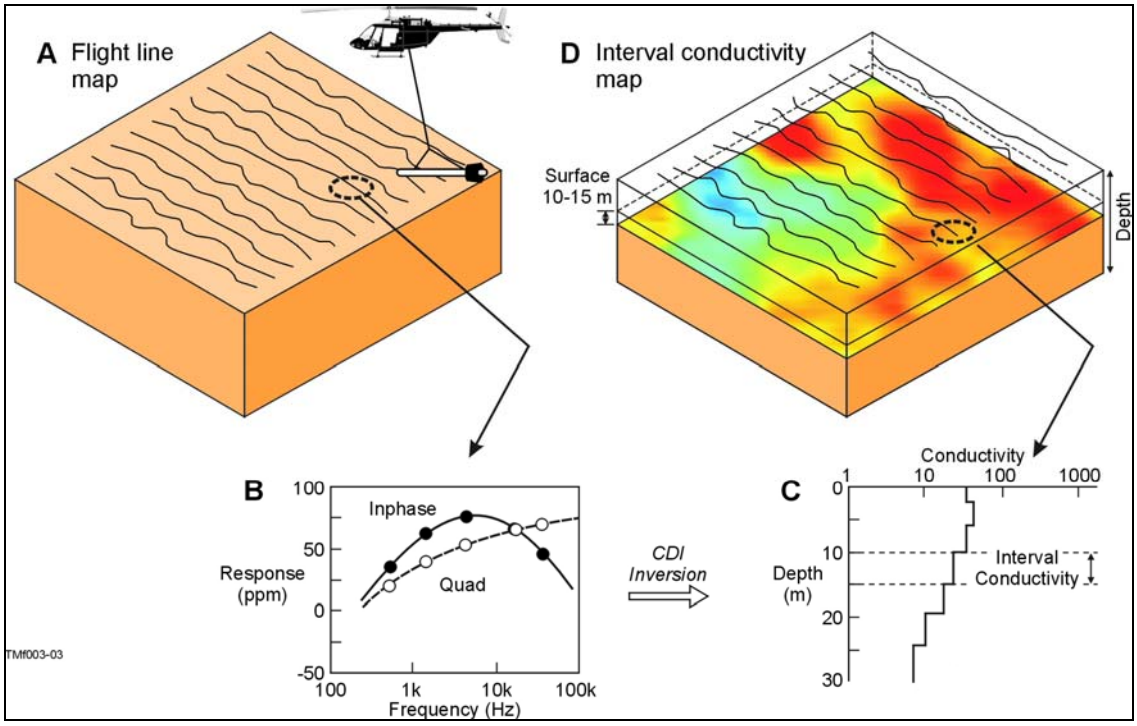

Figure 4: Schematic representation of Helicopter EM data acquisition and interpretation. A) Data are acquired along parallel flight lines; B) The receiver towed beneath the helicopter measures the inphase and quadrature electromagnetic response of the ground at several frequencies; C) The measured response is used to determine the conductivity-depth function by inversion. D) The conductivity-depth functions may represent layers are combined to produce an interpreted conductivity-depth sections and or interval conductivities which map the spatial distribution of conductivity as it varies with depth. (adapted from Fitterman and Deszcz-Pan, 2001)

This process is called inversion and makes use of nonlinear parameter estimation techniques (Deszcz-Pan et al., 1998; Ellis, 1998). Typically, parameters for two-, and sometimes, three-layer models can be estimated. In the studies at Riverland and Tintinara we were attempting to model 4 to five layers, although this was made possible by using constraints for some of the layers. Noise in the data, however, often produces large misfits between the measured and observed electromagnetic response, requiring the thinning of some of the inversion models. To minimize this problem, and to produce data

of a consistent quality suitable for inversion, required careful consideration of calibration issues. In the case of RESOLVE data for Riverland and Tintinara East we were attempting to generate maps of layers (eg clay-rich sedimentary units) that varied in conductivity and thickness. We were also making use of the CDI transform which permits the presentation of conductivity-depth models as stitched sections or as interval conductivities (Lane and Pracilio 2001) such as described in Figure 4D.

4. CALIBRATION METHODOLOGY

The methodology employed in this study builds on the experience of Deszcz-Pan *et al.*, 1998, Lane *et al*., 2001 and Brodie *et al.,* 2003, in AEM calibration. Two sources of ground geophysical information were available for the calibration of the airborne data. These were down-hole logs measured with an AUSLOG A034 inductive downhole conductivity probe and ground transient EM measured with a NanoTEM instrument. There remain some questions over the ground TEM results, particularly in respect of the inversion, and as a consequence we have concentrated all our attention on using the down-hole measurements. It is likely that when these questions are resolved these other ground data will be usefully compared with coincident drill hole data.

The drill hole data was available from a downhole logging programs carried out by the Bureau of Rural Sciences in December 2002 and March 2003 (Jones and Spring 2003) for 57 holes. Of these 44 were in the Riverland area and the rest in the Tintinara area. A subset of these holes was selected for analysis based on their proximity to the HEM flight lines and their having been measured to sufficient depth to provide a realistic measure of the airborne response. Boreholes located more than 60m from a flight line and with a total conductance less than 2.1S were rejected.

The down-hole conductivity information was averaged over 1m intervals and the resulting layered earth model was used, with the observed bird altitude, as input to an EM forward modelling procedure to estimate the expected airborne response. The holes that were used, with the observed and the modelled responses are tabulated in the Appendix 1.

The forward models were calculated using a layered earth forward modelling program developed at Geoscience Australia. The code is based on the formulation of Wait (1982) for the frequency domain response of vertical and horizontal magnetic dipole sources over a horizontally layered medium. Evaluation of the Hankel transforms was achieved via the filter coefficients derived by Guptasarma and Singh (1997).

The most appropriate model for correcting the data has been discussed by Deszcz-Pan *et al*., (1998). They suggest that the observed data is the result of multiple gain and offset distortions of the true data represented by the response predicted by the forward modelling.

Thus for observed In-phase and Quadrature data, X_i and X_q with complex representation $X= X_i + jX_q$ and modelled data $M= M_i + jM_q$ then

$$X = Ge^{j\phi}(M + B)$$

Here $Ge^{j\phi}$ is a complex gain and phase correction and B is a complex bias correction. In their formulation ϕ, B_i *and* B_q are parameters that change on a per-flight basis while G is constant for the whole survey.

In our analysis to-date we have only attempted to correct for the amplitude-scaling factor G. It remains to be seen if further correction on a flight-by-flight basis is necessary. This will only become apparent if the inversion results change substantially as a function of flight number. If this is the case, the per-flight correction factors will have to be estimated on the basis of the inversion miss-fits because there will not be enough ground geophysical information to estimate corrections for each of the 89 flights.

5. RESULTS

The following figures show scatter plots of the modelled responses verses the observed data (Figure 5 a to f). The results from the Riverland drill holes are shown as red dots while those from Tintinara are shown in mauve. The line of best fit is shown in red and its equation along with the R^2 value appears within each plot. The calibration parameter is, of course, the slope of the line of best fit.

If the data were correctly calibrated the modelled data would be expected to lie on the dotted, one-to-one line shown on the diagonal of each plot. Both Quadrature and In-phase responses are plotted on the same diagram. We considered the need for separate calibration for each but, in addition to this being hard to justify on the an understanding of the measurement process, the data sets did not warrant this extra complication. It is clear that there are significant deviations from correct calibration with a general trend to increasing calibration coefficients with increasing frequency.

The calibration factors determined from these Figures are summarized in Table 4.

Table 4: Calibration factors for the correction of RESOLVE HEM data for Riverland and Tintinara East

Frequency (Hz)	385.	1518.	3323.	6135.	25380.	106140
Calibration Factor	0.96	1.04	1.11	1.15	1.29	1.23

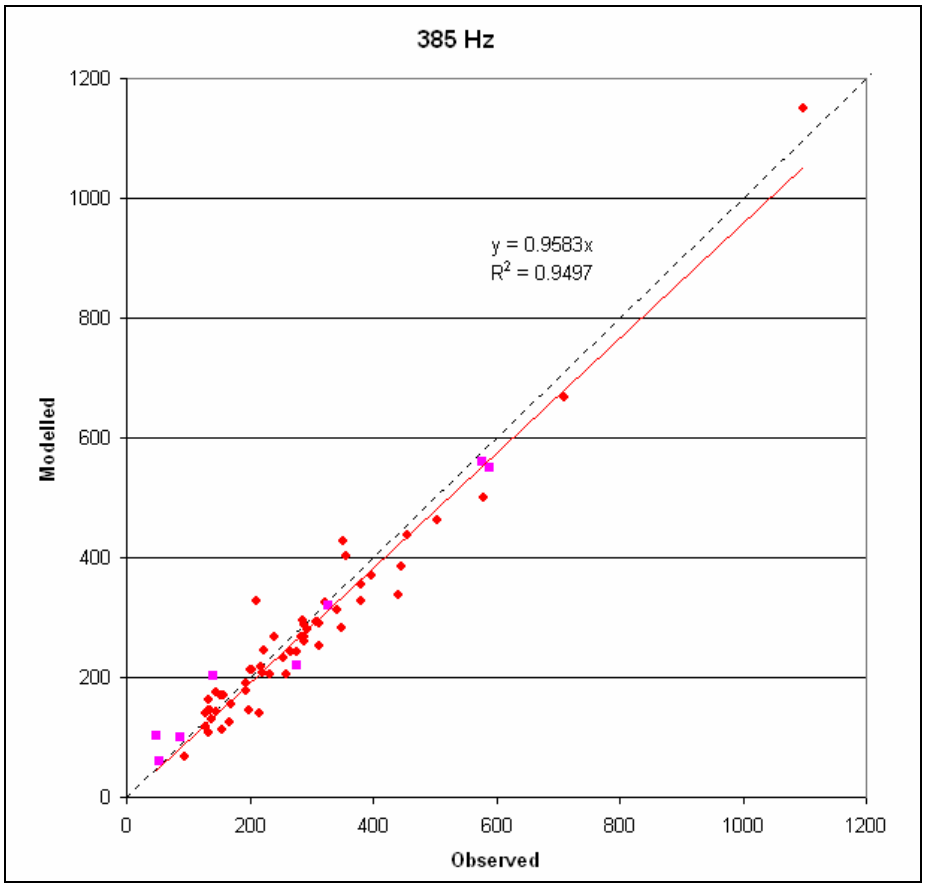

Figure 5a.: Calibration data for the 385 Hz, Horizontal Coplanar data

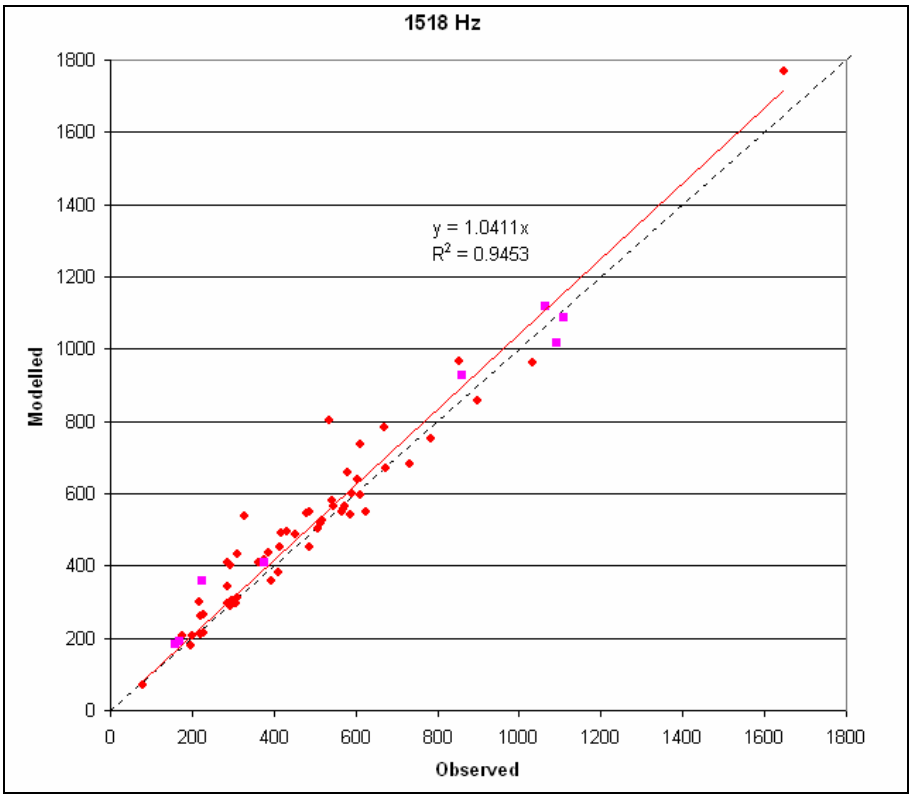

Figure 5b.: Calibration data for the 1518 Hz, Horizontal Coplanar data

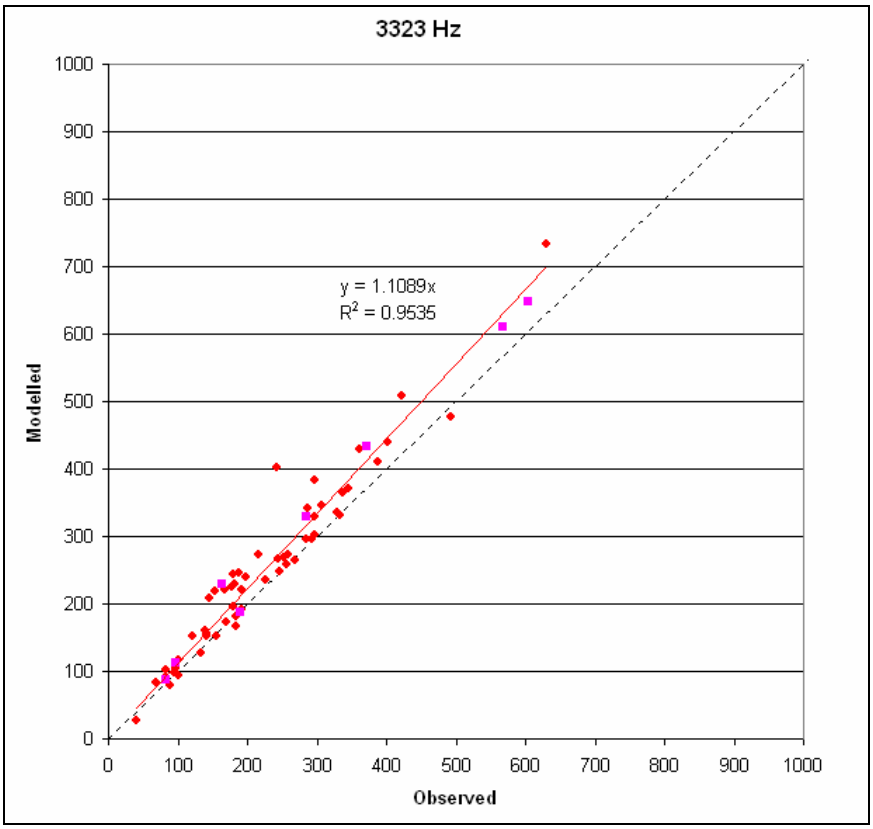

Figure 5c.: Calibration data for the 3323 Hz, Vertical Co-axial data

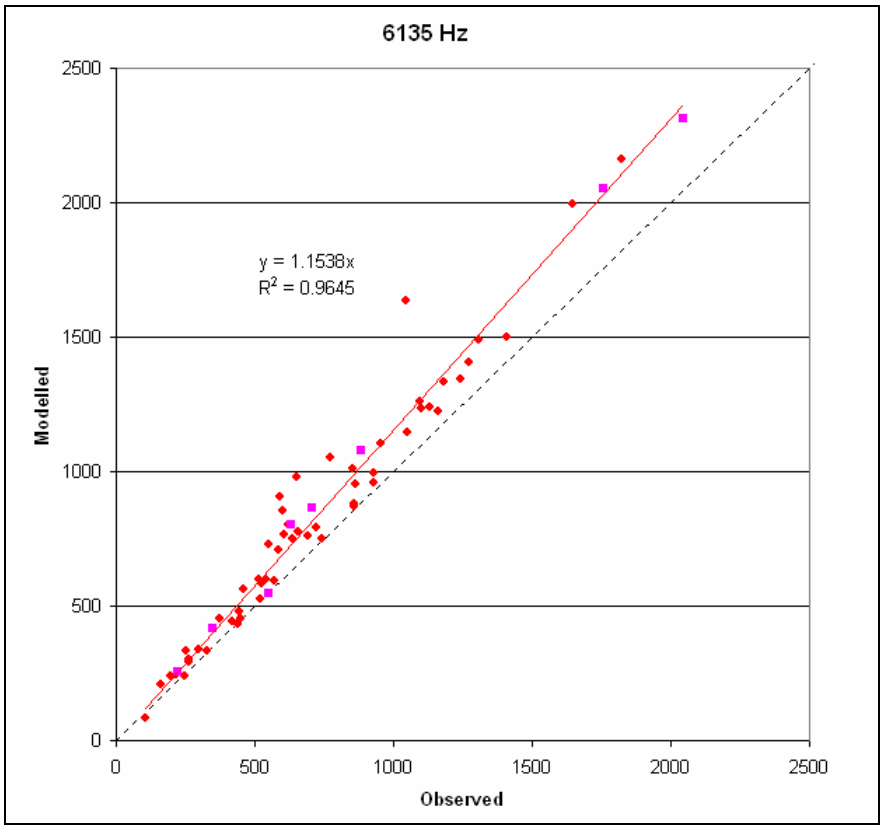

Figure 5d.: Calibration data for the 6135 Hz, Horizontal Coplanar data

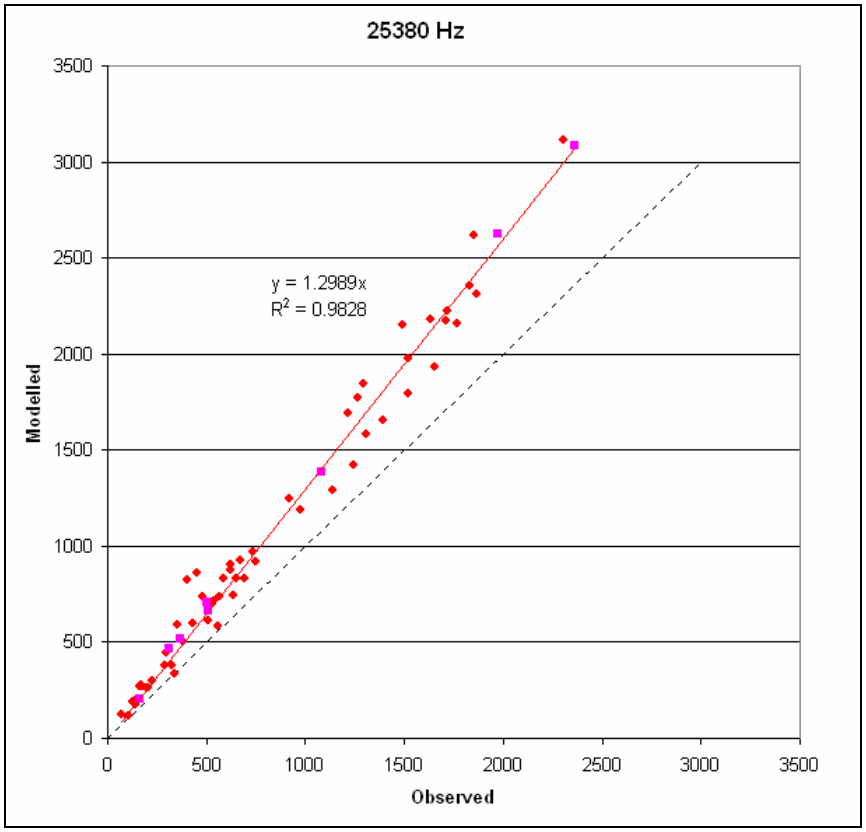

Figure 5e.: Calibration data for the 25380 Hz, Horizontal Coplanar data

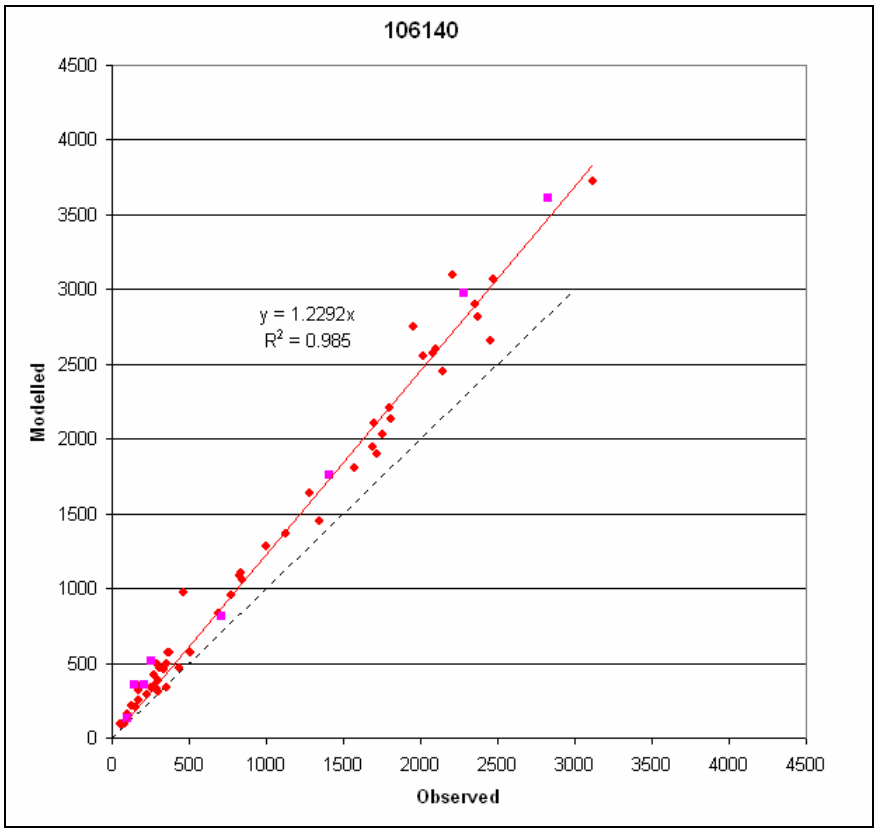

Figure 5f.: Calibration data for the 106140 Hz, Horizontal Coplanar data

In this analysis it has been assumed that the EM data are in error and must be rescaled. However it is possible that a similar miss-fit between modelled and observed data could be obtained if the measurement of the bird altitude was in error. High frequency data increases more rapidly than low frequency data as the altitude is decreased. Consequently, if the true altitudes had been greater than those measured, our modelled results would have been lower, better matching the observed data. This was checked by remodelling the data with an increased altitude and it was found that an increase in 1m could bring the high frequency data into calibration and required the low frequency data to have calibration factors of the order of 0.8.

In order to check this possibility we compared the apparent helicopter-to-bird cable length, which can be estimated in two ways. The first measurement is obtained by subtracting the elevations measured by the GPS systems (corrected for instrumental displacements) on the helicopter and the bird and the second is derived from the difference between the radar altimeter on the helicopter and the laser altimeter on the bird. The average of these differences for each of the approximately 600 lines of the survey is shown below.

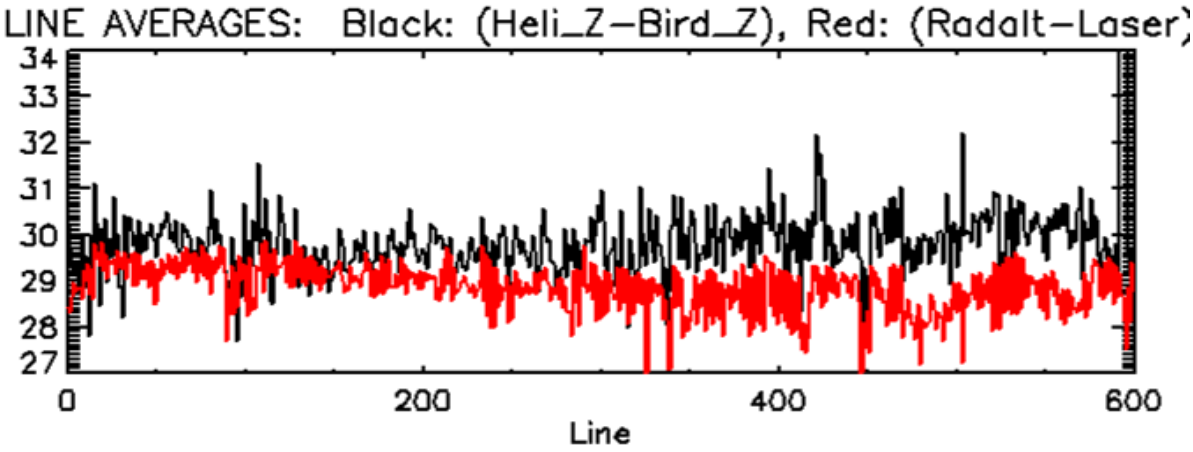

Figure 6: Line averages for the helicopter to bird cable length estimated from differences noted between GPS derived height measurements made on the helicopter vs. those measured on the bird (black line), and those determined from differences between the altitude of the helicopter (determined from a radar altimeter) vs the height of the bird (determined from lasar altimeter) (red line).

The two measures are systematically different but the error is not consistent with a laser altimeter that is reading too low. Any increase in the laser altimeter (the measure used for the modelling) will only increase this discrepancy. Thus although the cause of this discrepancy is unresolved it is unlikely to be indicative of the type of laser altimeter error we would expect on the basis of the calibration results.

These results, coupled with the fact that the laser altimeter is usually a reliable measurement led us to discount the idea that it was the cause of the calibration mismatch.

6. CONCLUSIONS

The RESOLVE data for the Riverland and Tintinara East surveys were recalibrated using borehole induction conductivity logs before any detailed interpretation of inversion was conducted. The calibration factors varied for each frequency. Significant deviations from an observed ground response as defined in the borehole data were noted. A general trend of increasing calibration coefficients with increasing frequency was recorded. The RESOLVE data were adjusted accordingly prior to their inversion.

7. ACKNOWLEDGEMENTS

Richard Lane has been of immense help in clarifying the issues involved in the calibration of this data and we are very grateful to him for his time and expertise.

We are also grateful to Steve Barnett of DWLBC and John Spring of the BRS for their assistance in acquiring and processing the borehole geophysical data used in this study.

This study was made possible through funding support by the South Australian and Commonwealth Governments through the National Action Plan for Salinity and Water Quality, and CRCLEME.

8. REFERENCES

Cowey, D., Garrie, D., and Tovey, A., 2003, Riverland and Tintinara, South Australia, RESOLVE Geophysical Survey, Acquisition and Processing Report. Report to the Bureau of Rural Sciences, available from Geoscience Australia.

Brodie, R.C., Lane., R., and Gibson, D., 2003, Gilmore Project, comparison of AEM and Borehole Conductivity Data: Report prepared for CRCLEME June 2002.

Guptasarma, D., and Singh, B., 1997, New digital linear filters for Hankel J0 and J1 transforms, Geophysical Prospecting, 45, 745-762.

Deszcz-Pan, M., Fitterman, D.V., and Labson, V.F., 1998, Reduction of inversion errors in helicopter EM data using auxiliary information, Exploration Geophysics, v. 29, p. 142-146.

Ellis, R., 1998, Inversion of airborne electromagnetic data, Exploration Geophysics, v. 29, p.121-127.

Fitterman, D.V., and Deszcz-Pan, M., 2001, Using airborne and ground electromagnetic data to map hydrologic features in Everglades National Park, in Proceedings of the Symposium on the Application of Geophysics to Engineering and Environmental Problems SAGEEP 2001, Denver, Colorado, Environmental and Engineering Geophysical Society, p. 17 p. including 9 figs. (on CD-ROM).

Jones, G & Spring, J. 2003, Report on downhole geophysical logging of bores in the Riverland Region, SA for the SA-SMMSP. Bureau of Rural Sciences, Canberra 2003.

Lane R., and Pracilio, G., 2000, Visualisation of sub-surface conductivity derived from airborne EM, EEGS SAGEEP Proceedings, Washington, 101-110.

Lane, R., Heislers, D., and McDonald, P., 2001, Filling in the gaps – validation and integration of airborne EM data with surface and subsurface observations for catchment management – an example from Bendigo, Victoria, Australia. Exploration Geophysics, 32, 205-215.

Munday, T., Brodie, R., Green, A., Lane, R., Sattel, D, Cook, P., Barnett, S., and Walker, G. 2003, Developing recharge reduction strategies in the Riverland of South Australia using airborne electromagnetic data – a case study in tailoring airborne geophysics given a particular target and a desired set of outcomes. Extended Abstracts ASEG 16th Geophysical Conference and Exhibition, February 2003, Adelaide.

Wait, J., R. Geo-Electromagnetism. Academic Press, New York, 1982.

APPENDIX

This table presents the results of the forward modelling as described in section 2.. Only those holes within 60m of a flight line and with a total conductance greater than 2.1S have been included in the analysis. In-phase results are on the first line for each hole and Quadrature results on the second.

	Observed Data						Modelled Data					
Hole ID \ Frequency	**385-**	**1518**	**3323**	**6135**	**25380**	**106140**	**385**	**1518**	**3323**	**6135**	**25380**	**106140**
RIV6HC	307.6	668.7	362.2	1307.5	1721.5	2211.3	293.1	781.4	428.7	1487.6	2226.4	3093.9
	355.8	580.4	258.4	722.4	452.4	461.9	403.7	660.1	272.6	793.6	857.3	972.2
RIV2LC	133.6	329.9	242.5	1046.8	1852.1	2475.6	106.5	536.8	401.1	1633.9	2616.5	3070.5
	209.7	535.8	297.1	954.7	636.3	275.7	326.3	800.9	382.3	1104.7	742.1	423.1
RIV5HC	216.7	565.1	306.7	1133.3	1392.3	1693.6	140.8	548.3	346.0	1240.0	1656.9	1946.1
	286.1	542.8	225.3	570.0	292.4	255.4	295.8	581.7	235.3	594.0	377.2	336.3
RIV2HC	158.4	611.1	422.9	1647.4	2307.8	3119.1	169.8	735.6	508.8	1994.0	3115.4	3724.0
	352.7	853.9	401.9	1096.7	620.8	370.3	428.4	965.6	440.2	1262.3	907.2	574.4
PYP14	289.6	571.7	328.8	1243.6	1869.8	2369.9	268.5	558.3	334.6	1341.7	2308.1	2817.4
	312.4	545.1	285.5	863.3	479.0	358.0	289.7	565.3	295.5	953.8	738.1	500.0
RIV3-1HC	446.7	1032.2	492.6	1406.7	1523.5	1750.5	386.0	962.1	476.6	1500.0	1791.1	2027.3
	503.7	589.5	192.6	421.5	224.9	168.3	463.1	599.4	192.7	444.7	300.8	253.3
MTH9	133.3	216.2	146.0	592.1	1216.8	1703.4	144.2	299.7	207.7	904.3	1694.1	2107.4
	132.9	293.5	181.6	637.7	507.9	301.3	162.8	400.2	229.2	751.5	611.5	383.0
PIEZO-Y	579.9	898.8	387.3	1271.0	1708.9	2016.3	501.0	855.5	411.1	1408.4	2174.5	2552.3
	396.7	432.7	191.1	587.1	354.0	162.7	371.2	495.2	221.5	706.9	587.2	355.4
PAG6	380.6	624.5	293.7	1052.9	1493.2	1956.1	327.5	550.8	296.0	1146.8	2153.9	2755.1
	313.0	416.1	188.8	599.7	402.0	333.2	253.1	451.2	245.4	855.1	821.3	456.6
PYP13	217.6	485.9	268.4	930.2	1140.0	1349.9	218.0	450.9	264.3	955.9	1287.9	1449.9
	258.7	410.0	170.0	450.5	194.9	152.6	206.2	383.5	172.1	453.8	259.2	204.3
RIV3PHC	456.9	782.7	334.3	928.9	977.4	1126.0	438.0	750.4	330.5	994.3	1192.0	1368.7
	342.4	296.8	95.8	215.4	145.2	104.4	311.7	304.3	97.6	242.8	206.2	152.2
PYP9	128.5	198.6	88.0	248.1	340.8	438.4	118.7	179.8	78.6	238.3	334.5	464.4
	94.6	79.6	41.4	105.9	105.3	55.7	68.6	70.0	27.6	84.3	119.7	94.7
PMA1	232.5	392.7	183.6	541.4	563.4	695.3	205.8	358.3	182.0	598.3	735.3	836.3
	199.7	200.0	69.2	162.3	67.5	79.5	144.2	207.5	83.5	205.9	126.0	99.4
PIEZO-3	152.3	362.9	178.0	619.8	916.5	1280.1	170.6	409.0	225.0	801.3	1250.0	1636.5
	202.6	287.8	121.7	373.7	300.4	286.5	212.4	341.3	152.5	453.2	442.7	329.1
PYP8	154.2	290.1	183.1	516.2	750.7	839.1	112.6	292.8	166.3	598.2	920.8	1105.6
	170.3	221.4	101.3	296.5	204.3	152.7	153.8	260.1	115.7	337.7	264.1	209.3

	Observed Data						Modelled Data					
Hole ID \ Frequency	**385-**	**1518**	**3323**	**6135**	**25380**	**106140**	**385**	**1518**	**3323**	**6135**	**25380**	**106140**
PIEZO-2	136.2	417.3	286.1	1181.4	1770.1	2452.5	146.2	490.3	341.6	1335.7	2159.8	2654.6
	240.4	604.8	297.0	859.4	521.7	312.2	268.0	640.3	302.2	878.2	692.4	471.6
PYP21	146.1	286.7	139.1	522.9	651.8	769.6	175.9	294.4	160.0	585.7	829.3	953.3
	168.3	220.0	96.0	263.4	130.3	103.0	125.3	210.0	104.1	299.6	187.0	155.5
PYP3	194.0	310.5	142.3	460.5	668.7	830.4	178.6	313.0	157.1	561.4	926.4	1086.8
	146.6	177.4	83.2	254.2	176.2	95.9	143.2	206.8	101.2	331.0	267.3	162.1
BKP16	379.6	612.6	251.7	858.1	1244.0	1574.0	355.2	595.5	268.9	870.1	1422.7	1806.4
	287.9	308.8	132.4	441.0	383.6	171.6	260.6	296.9	127.9	430.7	505.7	318.6
PYP5	193.6	519.0	296.9	1159.8	1657.0	2085.4	188.8	526.3	328.8	1223.9	1930.2	2575.7
	292.8	573.2	256.5	740.6	534.2	367.6	280.6	563.1	257.6	747.4	717.3	572.6
LH041G	255.7	507.7	245.2	853.0	1521.6	2099.9	232.3	500.8	267.6	1008.9	1978.6	2599.6
	283.9	386.4	192.5	654.3	588.5	290.1	267.6	437.4	221.2	776.4	831.8	494.3
PAG60	1098.7	1649.6	630.8	1822.2	1834.0	2149.2	1149.2	1767.9	733.3	2159.2	2356.5	2454.3
	711.1	485.9	140.9	326.7	141.1	82.5	667.8	548.7	151.5	334.0	177.2	91.2
MRK15	348.9	588.2	246.5	690.9	737.4	997.3	283.2	542.0	248.6	761.7	970.0	1278.2
	277.4	227.8	82.5	195.5	170.8	228.2	242.1	265.4	90.9	240.7	276.9	292.9
PYP2	265.6	451.6	216.8	772.8	1292.7	1796.2	243.1	485.3	273.0	1051.0	1848.1	2207.1
	223.3	311.3	167.6	548.5	432.9	269.4	245.1	434.0	221.8	726.6	595.9	347.8
BKP18	321.4	731.4	338.0	1094.8	1632.3	2354.7	326.2	681.0	364.1	1261.6	2177.8	2901.2
	440.2	479.1	197.9	604.9	623.0	508.3	336.9	543.6	240.0	764.3	872.1	569.8
MTH8	128.1	293.3	155.2	518.8	691.2	843.9	140.9	289.1	152.5	525.1	833.6	1053.2
	138.2	229.6	101.2	261.7	166.0	125.7	129.4	215.4	94.6	289.7	272.0	211.4
MRK16	221.7	375.4	180.7	650.0	1266.6	1805.9	208.4	415.8	243.7	977.5	1774.7	2129.0
	200.7	287.8	153.4	552.9	557.4	298.8	213.6	409.3	219.3	727.7	586.5	305.6
GDN35	287.7	674.6	344.7	1100.4	1307.0	1716.5	288.4	669.1	370.9	1232.3	1584.5	1897.5
	310.7	514.9	178.8	443.4	323.2	350.3	292.1	517.6	195.3	477.7	377.1	339.9
TIN3HC	276.0	1091.5	603.8	2047.9	2361.9	2828.2	220.9	1017.6	648.2	2314.0	3082.8	3607.5
	589.4	1065.7	372.1	883.5	503.1	258.2	551.1	1118.2	432.8	1080.4	710.2	518.4
MKN-20	54.2	159.1	97.3	347.0	507.2	707.1	58.9	182.0	112.7	418.6	663.0	813.9
	86.3	169.8	82.5	219.7	165.5	96.6	100.0	192.8	88.4	255.4	206.2	131.2
TIN4HC	327.4	1108.0	567.4	1759.5	1973.9	2280.3	319.6	1088.6	609.6	2050.2	2622.5	2977.6
	576.3	861.9	285.4	631.5	364.6	143.1	560.7	928.6	329.8	803.9	514.8	355.3
TIN5LC	48.1	224.6	163.7	708.4	1084.0	1413.2	102.0	358.0	229.2	863.7	1386.4	1760.8
	141.0	378.2	188.9	551.1	314.2	205.7	201.7	410.8	187.7	547.2	470.0	351.9